*J. Fluid Mech.* (1983), *vol.* 135, *pp.* 261–282
*Printed in Great Britain*



# Stratified flow over three-dimensional ridges

By I. P. CASTRO,
Department of Mechanical Engineering, University of Surrey,
Guildford, Surrey GU2 5XH, U.K.

W. H. SNYDER†
Meteorology and Assessment Division, U.S. Environmental Protection Agency,
Research Triangle Park, NC 27711, U.S.A.

AND G. L. MARSH
Northrop Services Inc., Research Triangle Park, NC 27711, U.S.A.

(Received 4 October 1982 and in revised form 7 June 1983)

An experimental study of the stratified flow over triangular-shaped ridges of various aspect ratios is described. The flows were produced by towing inverted bodies through saline-water solutions with stable (linear) density gradients. Flow-visualization techniques were used extensively to obtain measurements of the lee-wave structure and its interaction with the near-wake recirculating region and to determine the height of the upstream dividing streamline (below which all fluid moved around, rather than over the body). The Froude number $F(= U/Nh)$ and Reynolds number $(Uh/\nu)$, where $U$ is the towing speed, $N$ is the Brunt–Väisälä frequency, $h$ is the body height, and $\nu$ is the kinematic viscosity, were in the nominal ranges 0.2–1.6 (and $\infty$) and 2000–16000 respectively. The study demonstrates that the wave amplitude can be maximized by 'tuning' the body shape to the lee-wave field, that in certain circumstances steady wave breaking can occur or multiple recirculation regions (rotors) can exist downstream of the body, that vortex shedding in horizontal planes is possible even at $F = 0.3$, and that the ratio of the cross-stream width of the body to its height has a negligible effect on the dividing streamline height. The results of the study are compared with those of previous theoretical and experimental studies where appropriate.

## 1. Introduction

The flow of a continuously stratified fluid over two-dimensional obstacles has been a subject of study for many years. Theoretical studies have generally been based on either small-perturbation, linearized types of model (Lyra 1943; Queney 1948; McIntyre 1972) or models that assume a steady flow with, generally, a particular form of the upstream boundary conditions, which results in a linear equation for the streamline displacements (Long 1953; Davis 1969). Using various obstacle shapes, both Long and Davis conducted experiments which, as far as the basic features of the lee-wave field behind the obstacles were concerned, demonstrated reasonable agreement with the predictions of 'Long's model'.

The important dimensionless parameters are $K = ND/\pi U$, $F = U/Nh$ and

† Permanent address: National Oceanic and Atmospheric Administration, U.S. Department of Commerce.

$\epsilon = \pi h/D$, where $U$ is the upstream velocity, $N$ is the Brunt-Väisälä frequency based on the upstream density gradient, $h$ is the obstacle height and $D$ is the flow depth ($\epsilon KF = 1$). For $n < K < n+1$, where $n$ is an integer $> 1$, the flow is subcritical with respect to the first $n$ lee-wave modes. Therefore upstream disturbances corresponding to these modes can occur. Wei, Kao and Pao (1975) experimentally observed these 'columnar' motions, which take the form of horizontal velocity profiles with sinusoidal structure in the vertical. Baines (1977) investigated the limitations of Long's model in some detail, showing how both instability in the lee-wave fields and upstream disturbances violate assumptions inherent in the model.

In the three-dimensional case, the upstream motions, which similarly must occur at low $F$, have much lower amplitudes because they can spread horizontally. However, the general problem of stratified flows over three-dimensional obstacles is more difficult to handle theoretically, and therefore less well understood. Only Crapper (1962) and, more recently, Smith (1980) have investigated the effect of changes in the spanwise aspect ratio of obstacles. Crapper extended his earlier (1959) linear theory of the flow over axisymmetric hills of low slope to elliptical hills, and demonstrated that, for a given hill height and streamwise length, increasing the hill (cross-stream) width generally leads to decreasing wave amplitudes on the flow centreline ($y = 0$, with $z$ vertical), whereas increasing the streamwise length in proportion to the width leads to increasing wave amplitudes. Ultimately, the amplitudes decrease again for 'long' hills. The results showed that the idea originally suggested by Corby & Wallington (1956) applies equally well in three-dimensional flows, i.e. that the largest-amplitude waves are produced when a 'resonance' between the mountain shape and the airstream occurs. Lilly & Klemp (1979) recently demonstrated that the atmospheric response 'tends to be a strong function of the shape, as well as the amplitude, of the terrain'. In particular, they showed that nonlinear wave steepening produces the most intense waves for terrain with a gradual upslope and steep downslope profile. There is apparently very little experimental verification of these various theoretical results.

For very low Froude number ($F \ll 1$), Drazin's (1961) nonlinear theory for axisymmetric hills can be used to deduce how strong the stratification must be in order for any given streamline to pass round rather than over a hill. Sheppard (1956) postulated that an air parcel can rise over a hill only if it has sufficient kinetic energy upwind to overcome the potential energy required to raise the parcel from its upstream elevation to the top of the hill through the density gradient. He presented a general integral formula that can be used to calculate the kinetic energy required for a parcel to *just* surmount a hill (i.e. all kinetic energy is converted into potential energy). His results can be written as

$$\tfrac{1}{2}\rho U^2(z_S) = g\int_{z_S}^{h}(h-z)\,(-\mathrm{d}\rho/\mathrm{d}z)\,\mathrm{d}z, \tag{1}$$

where $U$ is the velocity and $\rho$ is the potential density of the air parcel far upstream at elevation $z_S$, $g$ is the gravitational acceleration and $h$ is the hill height. The elevation $z_S$ may be considered a dividing-streamline height. That is, below $z_S$, the air parcel has insufficient kinetic energy to surmount the hill and it must pass round the sides; above $z_S$, it has sufficient kinetic energy to surmount the hill.

For a uniform approach flow with a linear density gradient, this formula reduces to

$$H_S/h = 1 - F, \tag{2}$$

which is similar to Drazin's (1961) theory

$$H_S/h = 1-\beta F, \tag{3}$$

where $\beta$ is a constant. It should be noted that Sheppard's argument neglects the action of pressure forces, so that strictly, as in Drazin's theory, this result is only valid as $F \to 0$, when $\beta = O(1)$.

Hunt & Snyder (1980) (hereinafter referred to as HS) recently reported an experimental study that broadly confirmed the implications of these theories, at least for an axisymmetric, bell-shaped hill with a uniform approach flow and a linear density gradient. More recently, Snyder *et al.* (1982) provided a convincing demonstration that Sheppard's integral formula is valid for a wide range of hill shapes and upstream density profiles.

Neither Drazin, Sheppard nor HS has investigated the effect of hill spanwise aspect ratio on the flow structure. At first it may appear that the criterion for determining the dividing-streamline height ($z_S/h = 1-F$) is inadequate for all aspect ratios. If the hill were 'needle-like', streamlines would easily pass around it, independent of $F$; if the hill were two-dimensional, all streamlines would pass over the top. However, in neutral flow, even for a 'needle-like' hill, all streamlines originating in the centreplane pass over the crest, even branches that were on the surface well upstream. The question, then, is: in a stratified flow, *can* all streamlines pass over the crest? At the other extreme of a two-dimensional hill, upstream blocking can occur under strong enough stratification, so that streamlines originating at the lowest levels upstream could not pass over the crest.

HS also investigated how the lee-wave structure affects separation behind a hill. Separation from the curved surface of the hill was boundary-layer controlled when the lee-wavelength $\Lambda$ was much larger than the hill length $L$, totally suppressed at lower Froude numbers that led to $\Lambda = O(L)$ and, for even lower $F$, controlled by the lee-wave field. In the last case, separation occurred just upstream of the first lee-wave trough. Further discussions and experimental data for a polynomial hill, cone and hemisphere were presented by Snyder, Britter & Hunt (1980, hereinafter referred to as SBH). While most full-scale situations in which lee waves are important arise from hills of low-to-moderate slope (so that separation is not inevitable), some hills or mountains (and certainly large buildings) are sufficiently steep on the downwind side that separation is virtually fixed by the obstacle geometry. In these situations, the lee-wave field can presumably alter the size of the separated region, but cannot suppress separation altogether. Further, because real hills (and buildings) have finite spanwise aspect ratios, the effect of the lee-wave field must in practice depend not only on $F$ (even an $F$ based on hill *length*), but also on the spanwise shape of the hill.

The work described here was undertaken to investigate these various flow features as a function of hill spanwise aspect ratio. The experimental methods used are described in §2; the major results are presented in §3. Although many of our conclusions are rather qualitative, the use of flow-visualization techniques allowed a number of quantitative measurements to be made. We believe these results are not only interesting and instructive in their own right, but also help to broaden the current understanding of three-dimensional stratified flows.

## 2. Apparatus and techniques

All the experiments were conducted in a large towing tank, 1.2 m deep, 2.4 m wide and 25 m long, at the EPA Fluid Modeling Facility. Details of the tank, the towing

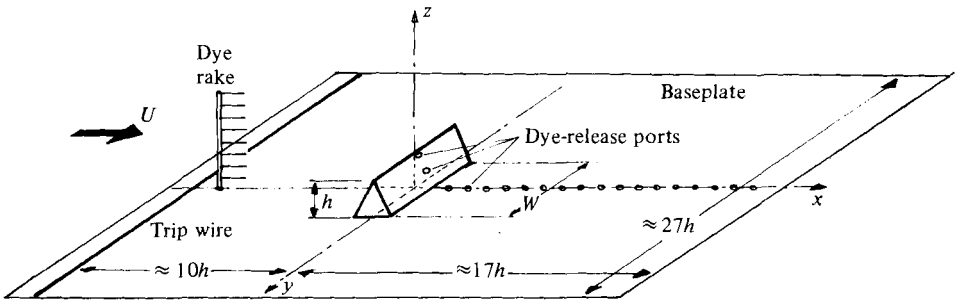


FIGURE 1. Sketch of experimental arrangement (not to scale).

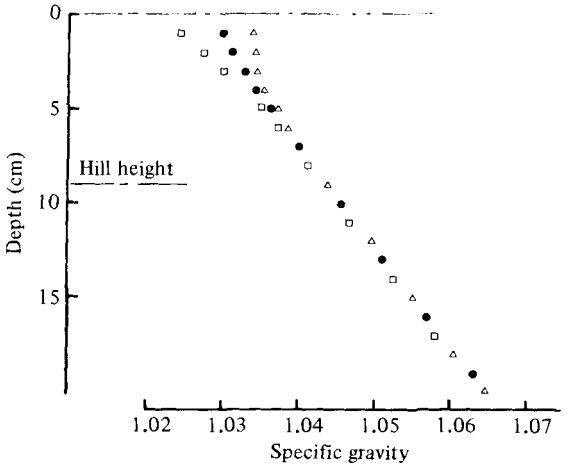


FIGURE 2. Surface-layer density variations: □, after initial fill; ●, after 5 tows; △, after a further 70 hours.

carriage and the filling system are given by Thompson & Snyder (1976) and HS. The hills, which were made of acrylic plastic, were mounted on a flat baseplate (see figure 1), suspended from the carriage, and towed upside-down across the water surface. The baseplate was immersed approximately 6 mm for each tow.

Salt water was used to obtain stable density profiles. For this study, linear profiles with nominal Brunt–Väisälä frequencies of 1.33 or 0.45 rad/s were used. Because the model height $h$ was less than half that used in the previous experiment of HS, erosion of the density profile at the surface was relatively more significant. Figure 2 shows how the linearity in the surface layer was degraded by five consecutive tows and simple molecular diffusion and evaporation over one weekend. Rather than refill the whole tank every few tows (or days), an additional layer of brine was introduced at the bottom, and the corresponding nonlinear layer at the top was removed by siphoning (skimming) whenever necessary. Figure 3 shows salinity profiles measured about two weeks apart, during which time 36 tows and 5 partial drains-and-refills (totalling about 22 cm depth) were made. The linearity and slope ($\propto N^2$) were well maintained during this period, although there was an increasingly thick region of fluid of nearly constant density accumulated at the bottom. We do not believe that this gradual change in the bottom boundary condition significantly affected the study results.

Because we wished to investigate the influence of lee-wave fields on recirculation

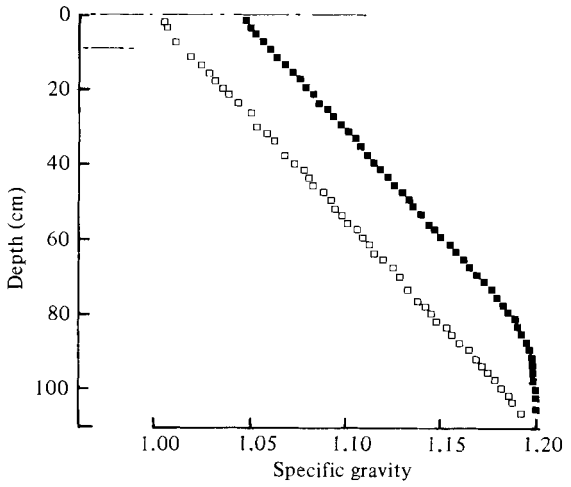


FIGURE 3. Complete density profiles: □, after initial fill; ■, after 36 tows and 5 partial refills (totalling approximately 22 cm).

regions without the complication of boundary-layer-controlled separations (and the consequent uncertainties about the influence of Reynolds number), the models used had triangular cross-sections with height $h$ = base-length. The spanwise width (between the vertical end faces) gave aspect ratios $\alpha$ ($= W/h$) between 1 and 8. The geometry therefore ensured fixed separation points at the apex of the ridges, although the windward slope was sufficiently steep to promote upstream separation in addition. The details of this latter feature of the flow varied substantially with aspect ratio in the stratified-flow cases (in contrast to the neutral flow cases). However, these variations did not significantly affect the qualitative nature of the downstream flow (see § 3.1).

Several considerations were pertinent in choosing the ridge height $h$. First, it was necessary to ensure simultaneously that the upstream pressure field did not influence the flow near the leading edge of the baseplate and that the recirculating region downstream did not extend beyond the baseplate. Secondly, it was necessary to ensure that the flow would be subcritical with respect to as many wave modes as possible, thus more closely simulating the 'infinite-upper-boundary' case. Therefore $\epsilon = \pi h/D$ had to be as small as practically possible. (In the HS experiment, $\epsilon = 0.65$, so that for $F = 1$ only one lee-wave mode was possible, rising to 3 at $F = 0.4$.) Moving the upper boundary as far away as possible also reduces the amplitudes of the possible upstream columnar motions; these are always more significant when upward radiation of energy is prevented by a 'rigid' lid at $D < \infty$ and wave reflection therefore occurs (Miles 1968; Baines 1979*a*).

Based on these considerations, a ridge height of 9 cm was selected, allowing about $10h$ upstream distance and $15h$ downstream on the baseplate (see figure 1); thus, even for $\alpha = 8$, no significant effects were expected from the ends of the baseplate. A double-sized version of the hill with $\alpha = 1$ was also constructed; with the 3:1 range in $N$, this enabled a 6:1 variation in Reynolds number at constant $F$ to be obtained. For the 9 cm hills, $\epsilon$ was about 0.26, which usually allowed the flow to be subcritical for at least 4 lee-wave modes when $F < 1$.

Two small holes were drilled on the rear face of each hill, one near the top and the other at $\frac{1}{2}h$, thus enabling coloured dye to be injected directly into the wake. Similar holes were placed in the baseplate at intervals of $\frac{1}{2}h$ along the flow centreline

($y = z = 0$) downstream of the hill. During each tow, dye that was slightly heavier than the surface layer was slowly ejected from these holes to form miniature 'plumes'. The motion of these plumes was carefully observed to establish reasonable estimates of the mean locations of centreline reattachment or separation points.

Considerable use was also made of a technique analogous to the surface oil-flow method used in wind tunnel studies. Before starting a tow, a line of blue dye slightly lighter than the surface layer was laid spanwise across the baseplate near the leading edge. With suitable adjustment of the density difference (which had to be adjusted for different towing speeds), this dye line was swept downstream past the hill, eventually delineating quite clearly the upstream separation line and, often, the three-dimensional separation behind the hill.

The shadowgraph technique, as used by HS to visualize the lee-wave structure, was much less useful in this study, mainly because of the optical difficulties in lighting the necessary flow regions, which were much closer to the baseplate than they were for the considerably larger hill used by HS. However, extensive use was made of multiple dye streamers. These were injected on the centreplane ($y = 0$) at a distance $9.5h$ upstream of the hill and at height intervals of 2 cm to about $2.5h$ from the surface. The procedure for ensuring that each streamer initially had the same density as that of its surroundings was described by HS.

Because the detailed characteristics of the flow near the hill were expected to depend partly on the nature of the upstream boundary layer, a fairly substantial tripwire (5 mm) was positioned about 5 cm from the leading edge of the baseplate. This tripwire ensured a turbulent boundary layer for all neutral flow cases, but stratification prevented transition for $F < 0.6$. Possible effects of this are discussed later.

Still photographs and/or motion pictures were taken at nominal Froude numbers of 0.2, 0.4, 0.6, 0.8, 1.0, 1.3 and 1.6 for each hill, using all the flow-visualization methods (not necessarily simultaneously!); lighting arrangements were similar to those described by HS. Some 'baseline' experiments in neutral flow ($F = \infty$) were also conducted. Although many of our quantitative measurements of the *steady* flow phenomena are based on photographs, deductions, particularly those concerning the turbulent recirculating downstream regions, are based on copious notes made during visual observations of very many tows.

## 3. Results and discussion

### 3.1. *The upstream flow*

#### 3.1.1. *Dividing-streamline heights*

For these runs, a red dye streamer was placed at the dividing-streamline height predicted by (2); blue streamers were placed 1 cm above and below this height. According to the dividing-streamline concept, the upper streamer should pass over the hill, the lower one should pass round the sides, and the middle one should split. Visual and photographic observations were used to assess the accuracy of the $z_S/h = 1 - F$ result. Figure 4 presents the data for the two extreme-aspect-ratio cases ($\alpha = 1$ and 8). Although the experimental uncertainty was not insignificant, no trend with aspect ratio was evident. Estimates of $z_S$ from the *multiple* dye streamer experiments designed to highlight the lee-wave structure (see § 3.2 and e.g. figure 7) were broadly consistent with this result.

Figure 4, in conjunction with results of HS and SBH, illustrates that the

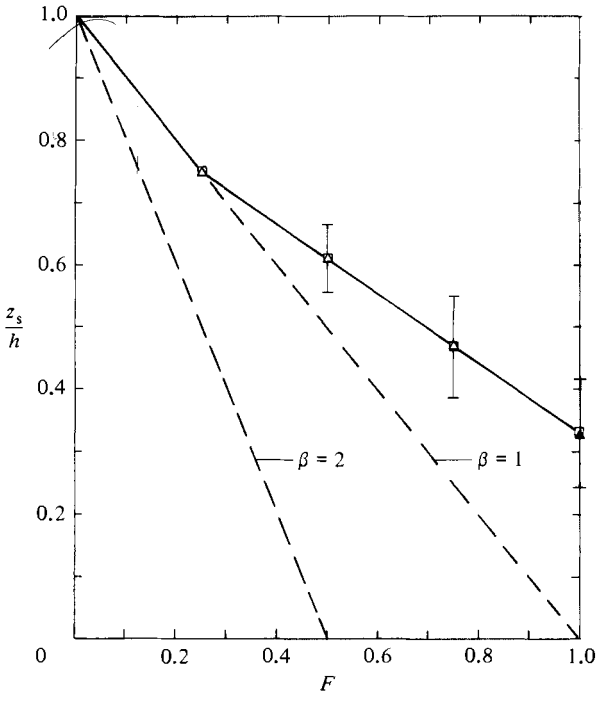


FIGURE 4. Dividing-streamline height; $\alpha$ = △, 1; □, 8. I, scatter bar. $\beta = 2$ line is Baines' (1979) smallest gap case ('$\alpha$' $\gg$ 8). $\beta = 1$ line is the $z_S/h = 1-F$ line.

dividing-streamline height follows the '$1-F$' rule for $F < 0.3$, but deviates significantly at higher Froude numbers. This is almost certainly due to the formation of an upwind vortex (see figures 8*c*, 11*a*) that produces some downwash on the front face of the ridge, so that some of the streamlines having sufficient energy to surmount the hill are, in fact, pulled downwards by the low pressure in the horseshore vortex and find it 'easier' to pass round the sides of the hill. In neutral flow, the upwind slope of the hill is sufficiently steep to promote upstream separation and a consequent vortex flow; this vortex only disappears at $F < 0.3$, when the flow becomes largely confined to horizontal motions. Note that the dividing-streamline concept only addresses the question of whether a particular fluid parcel *can* surmount the hill; even if it has sufficient kinetic energy to surmount the hill, if it is not on the (vertical) centreplane of the flow, it *may* go round the sides. This certainly happens with wind meander in the field and did happen with secondary flows in our towing tank experiments.

The only other relevant data is that of Baines (1979*b*), who studied the 'inverse' case of a nearly two-dimensional hill with an increasingly wide gap at one end between the hill and one sidewall of the towing tank. His method of determining $z_S$ is questionable because the dye was injected at various angles to the horizontal, and because, in general, it did not have the same density as the surrounding fluid at the height of injection. In the case of the smallest gap ($\frac{1}{16}$), the most closely two-dimensional case (largest $\alpha$ in present terms), Baines found $\beta \approx 2$, but with rather large error bounds of $1.6 < \beta < 2.4$. He also found that $\beta$ decreased sharply as the gap width increased, to a value of about 0.8 at a gap width of $\frac{3}{8}$. In the present study, the 'smallest gap width' (about $\frac{7}{10}$) was nearly twice as large as the largest gap width ($\frac{3}{8}$) in Baines' study, so that our results do not overlap with those of Baines. The simple energy arguments

of Sheppard (1956) worked well in the present case, provided that upstream vortex motions were not strong ($F < 0.3$). It seems that $\beta = 1$, whatever the shape of the hill, which is a very useful 'rule of thumb' for the full-scale situation of effluent sources upwind of hills. However, changes in stratification with height and velocity shear in the upstream flow may have significant effects on $\beta$ (see Snyder *et al.* 1982).

### 3.1.2. *Upstream separation*

Figure 5 shows a sequence of surface flow patterns for the $\alpha = 1$ hill with $F = \infty$, 1.0 and 0.8, and the $\alpha = 2$ hill with $F = 0.8$. For $F = \infty$, separation occurred at a distance $1$–$1.5h$ upstream for all $\alpha$; this distance increased slightly as the towing speed decreased sufficiently to cause the upstream boundary layer to be transitional or to remain laminar all the way to separation. Figure 5(*a*) is typical of the neutral flow cases in which a turbulent upstream boundary layer existed. No direct measurements of the upstream boundary layer were made, but on the basis of standard formulae for turbulent-boundary-layer growth in zero pressure gradient, its thickness at the location of the body but in its absence would have been about 3 cm (one third of the body height). For $F < \infty$ the tendency for this to increase because of reduced Reynolds number would be counteracted by the damping effects of the stratification. Under stratified conditions, separation occurred increasingly earlier as $F$ decreased and/or $\alpha$ increased. For example, figure 5(*d*) shows that separation occurred about $2.5h$ upstream. Figure 6 shows the data for all hills and includes the results for $F = \infty$. (In the latter case, the $F$-scale is effectively a velocity or Reynolds-number scale.) The boundary layer remained laminar to larger $Re$ as $F$ decreased, but this does not explain the very large upstream movement of the separation line as $\alpha$ increased. At $F = 1.0$, the boundary layer was always turbulent (and at $F = 0.4$ it was always laminar). However, for $\alpha = 8$, separation occurred nearly twice as far upstream as it did for $\alpha = 1$ (see figure 6). Some runs undertaken with the double-sized $\alpha = 1$ hill and/or different values of $N$ confirmed that these changes were not essentially caused by changes in Reynolds number.

A possible explanation is that, as $\alpha$ increased, the upstream-propagating wave modes (although still limited in extent by the three-dimensional nature of the flow) became stronger near the hill and, in particular, led to more extensive regions of blocking at the very lowest levels. This would lead to earlier separation. At very low $F$ (say $F < 0.4$) vertical motions became increasingly inhibited, so that the flow was more like the free flow over a vertical two-dimensional body (see §3.3) and the 'separation' line moved back towards the body again – it can perhaps no longer be described as a separation line in the usual sense.

The results presented in the following sections suggest that these movements of the upstream separation point did not significantly affect the structure of the lee-wave field or its interaction with the downstream recirculating region. Other flow features evident in figure 5 are discussed later.

## 3.2. *The lee-wave structure*

Typical photographs of the multilevel dyestreak patterns are shown in figures 7 and 8. Figure 7 demonstrates the effects of decreasing the Froude number while holding the hill aspect ratio constant. Figure 8 shows the effect of varying the aspect ratio while holding the Froude number constant. Quantitative measurements of lee wavelengths and amplitudes were deduced from such photographs; direct visual observations showed that these quantities were essentially steady throughout any

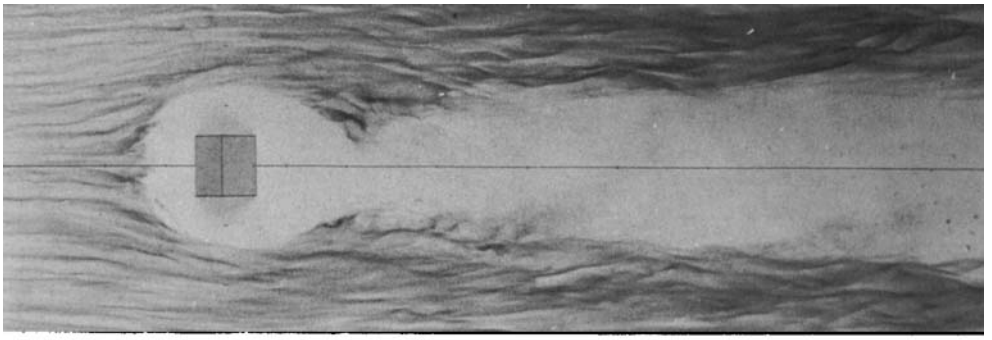

(*a*) Neutral flow, $\alpha = 1$

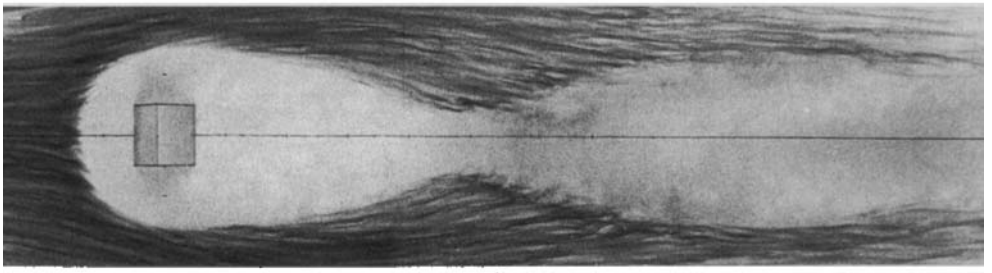

(*b*) $F = 1.0$, $\alpha = 1$

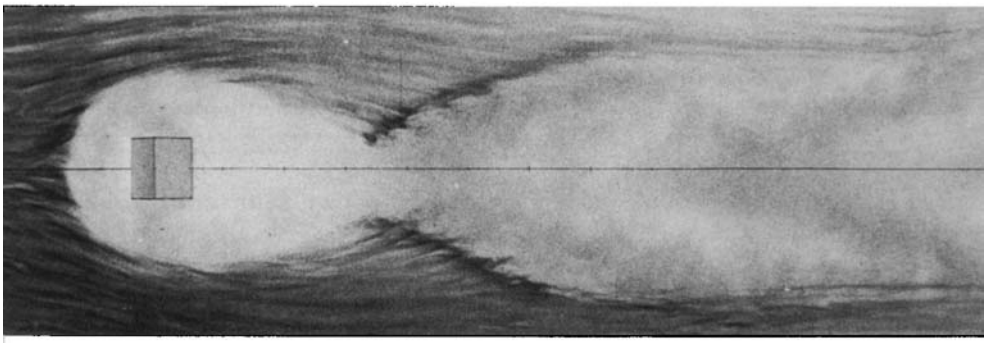

(*c*) $F = 0.8$, $\alpha = 1$

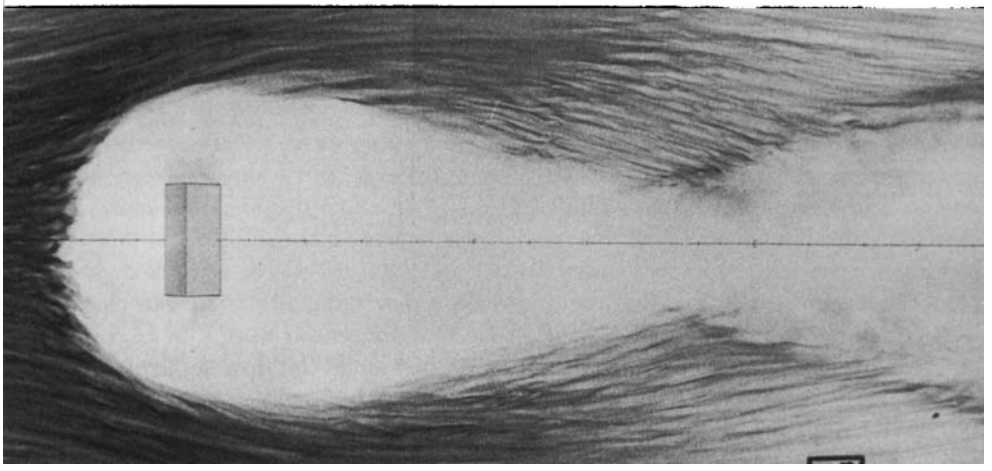

(*d*) $F = 0.8$, $\alpha = 2$

FIGURE 5. Surface flow patterns.

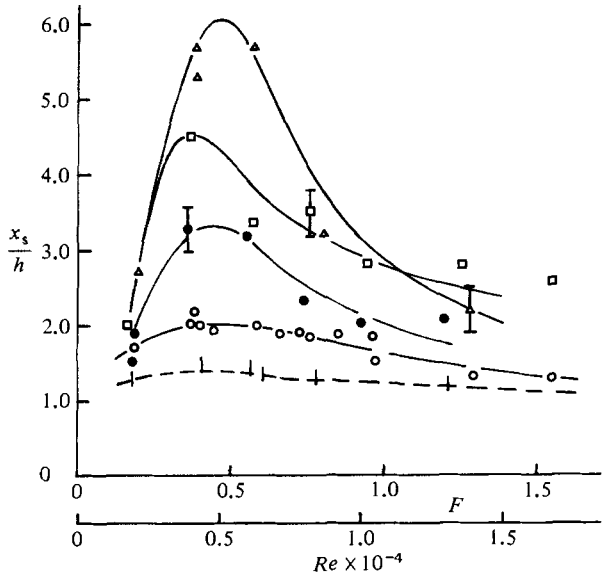


FIGURE 6. Location of separation line (on $y = 0$) upstream of hill. ○, $\alpha = 1$; ●, 2; □, 4; △, 8. $-+-$, $F = \infty$, all $\alpha$ (use $Re$-scale). I, typical scatter bar.

tow, unless wave breaking occurred (see later discussion). The wavelength data are presented in figure 9.

With Long's (1953, 1955) assumptions, principally that $\rho U^2$ is constant with height far upstream, the well-known equation governing streamline displacement $\delta$ is

$$\nabla^2\delta + k_0^2\delta = 0, \tag{4}$$

where $k_0^2 = N^2/U^2$. From this equation, it may be shown that, in two-dimensional flows, stationary lee waves exist only when

$$(k_0^2 - k_n^2)^{\frac{1}{2}} = \frac{n\pi}{D}, \tag{5}$$

where $n$ is a positive integer and $k_n$ is the wavenumber $2\pi n/\Lambda$. The first lee-wave mode therefore has a wavelength $\Lambda$ given by

$$\frac{\Lambda}{h} = \frac{2\pi F}{(1-\epsilon^2F^2)^{\frac{1}{2}}}.$$

Three-dimensional waves have a complicated structure, of course, but analysis indicates that lee waves have crests which diverge only slowly from the $y = 0$ direction and the wavelength is the same as in the two-dimensional case, even for bodies with small aspect ratios. Wave kinematics shows the additional possibility of diverging waves, like ship waves on deep water (Scorer 1978; Gjevik & Martinsen 1978). The results in figure 9 show that the axial wavelength $\Lambda$ was close to the two-dimensional 'limit' for all $\alpha$ at $F < 1$. As $\alpha$ increased and $F > 1$, $\Lambda$ increased above this limit. In our experiments, $\epsilon = 0.26$, but since the flow separated from the ridge top, producing a wake whose height was somewhat greater than $h$, the effective $\epsilon$ may have been somewhat larger. The theoretical relation for $\epsilon = 0.4$ (i.e. taking the effective height to be about $1.5h$) is included in the figure and, within experimental uncertainty, the data are quite close to that result. Alternatively, the change in $\Lambda$ with $\alpha$ at larger Froude numbers may be a result of the influence of the tank side-

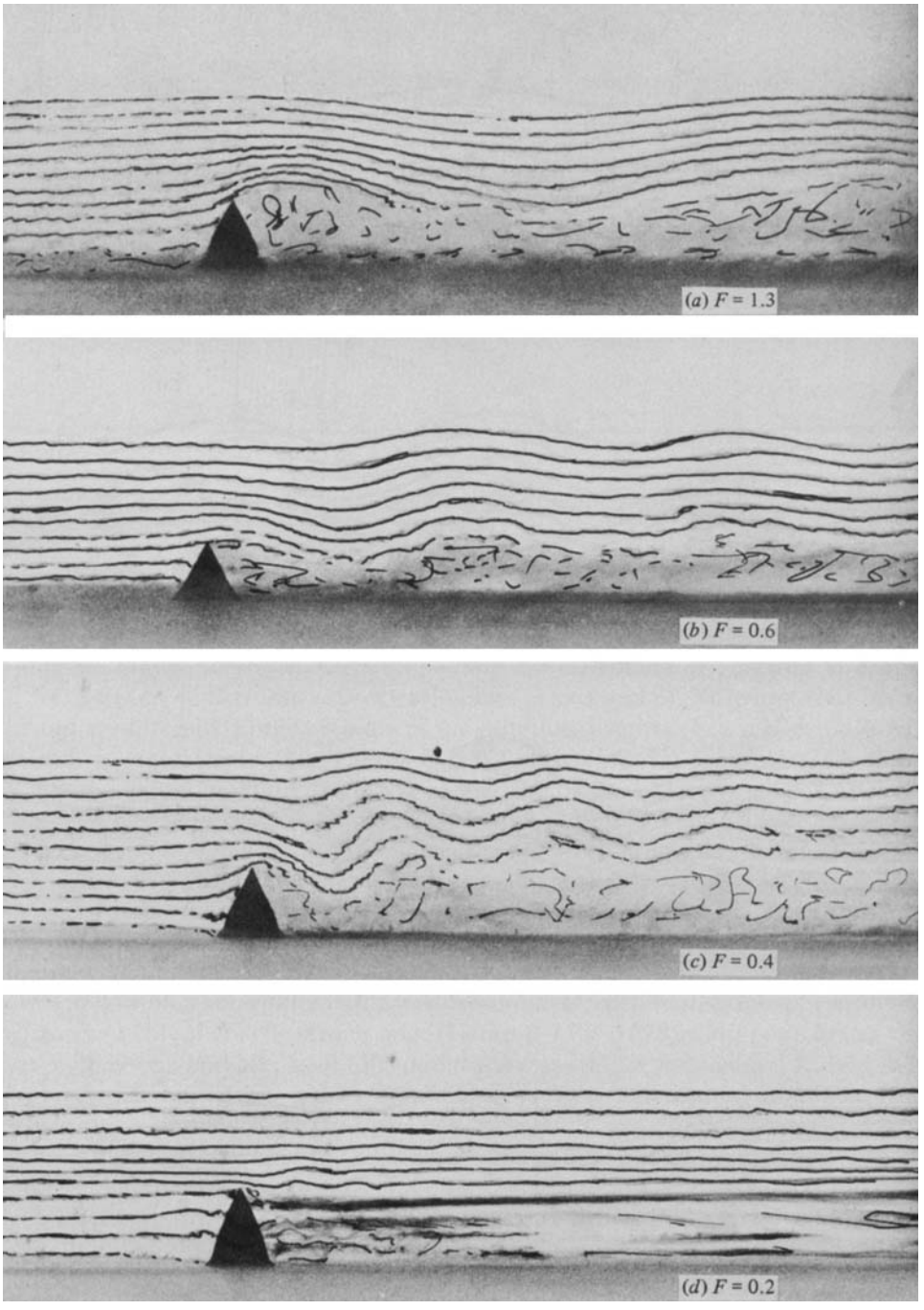


FIGURE 7. Dye streaks for $\alpha = 1$ ridge. Dye streaks 'touched up' for clarity.

walls; for $\alpha = 4$, the width $W$ of the body was about 20 % of the tank width and 40 % of the tank depth.

Figure 10 shows how the wave amplitude (trough-to-peak height), measured for the first wave behind the hill occurring in the dye streamer originating at $z/h = 2.4$ (the 'top' streamer in the photographs), varied with $F$ and $\alpha$. For $\alpha > 4$, wave

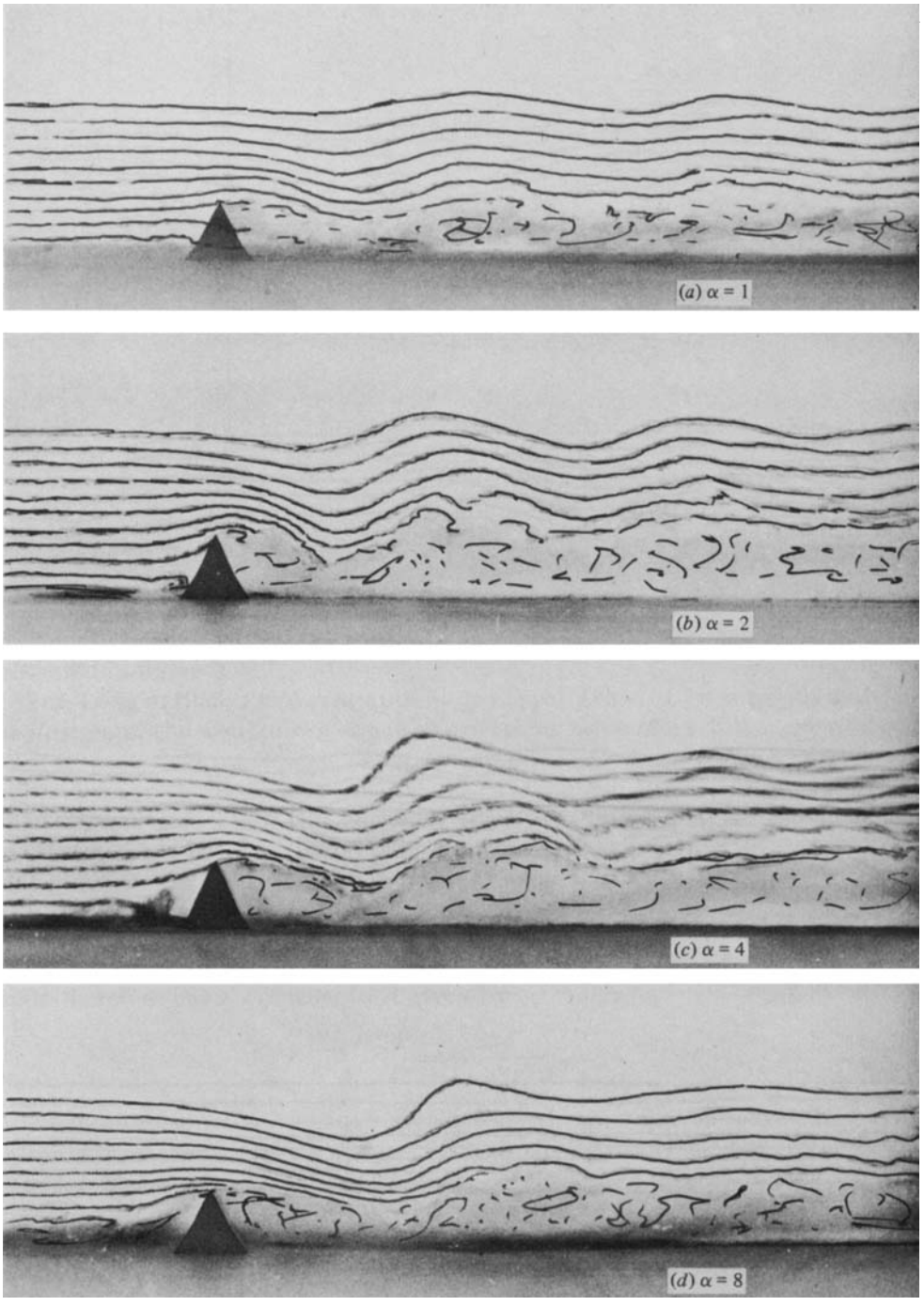


FIGURE 8. Dye streaks for $F = 0.6$.

breaking occurred when $0.3 < F < 0.5$. The vertical height at which this turnover occurred depended on both $F$ and $\alpha$. For example, for $\alpha = 4$ and $F = 0.4$, breaking occurred below $z = 2h$, so the top streamline did not break but had a much lower amplitude than if breaking had not occurred (see figures 11*a*, 12). In contrast, for $\alpha = 8$ and $F = 0.4$, the top streamline ($z = 2.4h$) was directly involved in the

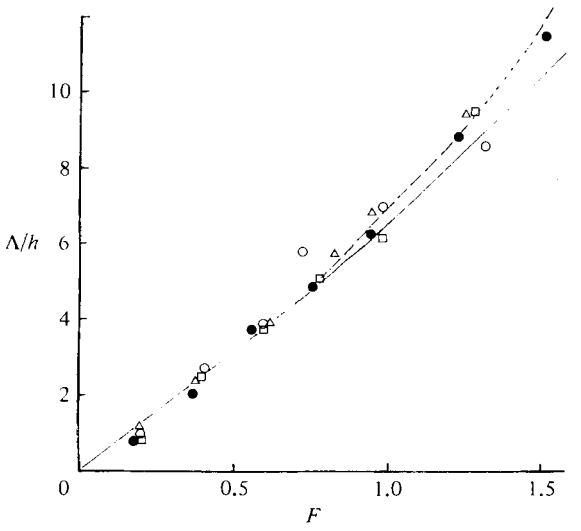


FIGURE 9. Lee wavelengths: ○, $\alpha = 1$; ●, 2; □, 4; △, 8. Lines are the two-dimensional result; $\Lambda/h = 2\pi F/(1-\epsilon^2F^2)^{\frac{1}{2}}$; ——, $\epsilon = 0.26$; – – –, 0.4.

breaking instability, so that a wave amplitude measurement was not possible (see figure 11*b*).

Wave breaking depends, of course, on the maximum wave slope, rather than the amplitude. Figure 13 shows wave-slope data for streamers originating at $z/h = 1.6$ and 2.4, for the two extreme-aspect-ratio cases ($\alpha = 1$ and 8). Note first that breaking occurred at different Froude numbers for different heights. For $\alpha = 8$, no breaking occurred up to at least $z/h = 1.6$ for $F = 0.4$; breaking did occur at $z/h = 2.4$. For $F = 0.2$, however, breaking occurred at $z/h = 1.6$, so that wave slopes above that region were much smaller. Secondly, it is clear that for $\alpha = 1$ the wave slope decreased with increasing height for all $F$, whereas, for $\alpha = 8$, the reverse was true, at least up to $z/h = 2.4$. Figure 14 shows how the wave slope at $z/h = 1.6$ varied with $\alpha$ at fixed values of $F$, and it is clear that the lee-wave field can be 'tuned' by changing the hill aspect ratio. This appears to be the first laboratory evidence for three-dimensional bodies that supports the theory (Corby & Wallington 1956) that the hill shape and upstream flow characteristics can cause 'resonance', although atmospheric evidence in support of this theory is strong (e.g. Klemp & Lilly 1978). Crapper's linear theory for axisymmetric and elliptical hills demonstrates similar behaviour; Lilly & Klemp (1979) provide the most recent example of a two-dimensional nonlinear theory showing the same effect. If Crapper's (1959) results are applied to an obstacle for which, in his notation, $H/a = 2$ (corresponding roughly to our $\alpha = 1$ body) then the calculated lee-wave slope at a given height as a function of $F$ is very similar to the curves in figure 13, although of rather lower amplitude. Peak wave slopes occur around $0.2 < F < 0.4$, as they did in our experiments. This is an extrapolation of Crapper's results far beyond the strict limits of linear theory (for which $H/a \ll 1$, $F \gg 1$) but it does suggest that the same mechanism of 'tuning' is operating,† namely a correspondence between the lateral dimensions of the obstacle and the lee-wave lengthscale $U/N$.

† One might reasonably ask (as a referee has done) about the extent of this 'tuning' effect on the lee wave field. Further experiments, yet to be fully analysed, have indicated that, because the wave amplitude always decays fairly rapidly with $y$ (and $x$), wave breaking tends to be fairly localized. When breaking does not occur, amplitudes are everywhere rather greater than when the flow is 'detuned'.

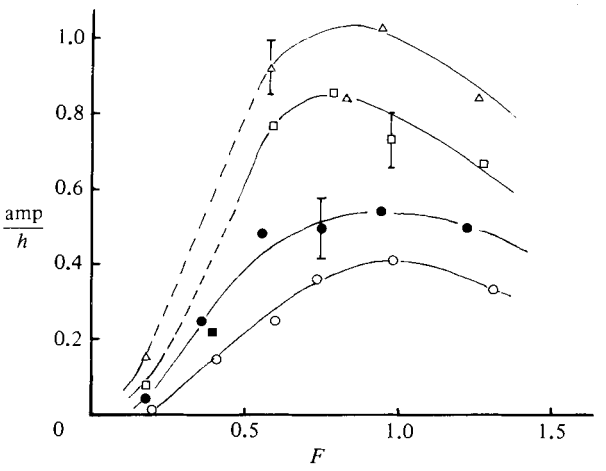


FIGURE 10. Amplitude of first wave shown by streamer originating at $z/h = 2.4$. ○, $\alpha = 1$; ●, 2; □, 4; △, 8. ■, as for □, but with a breaking wave at a lower level (figure 11*a*). Dotted lines show regions of wave breaking.

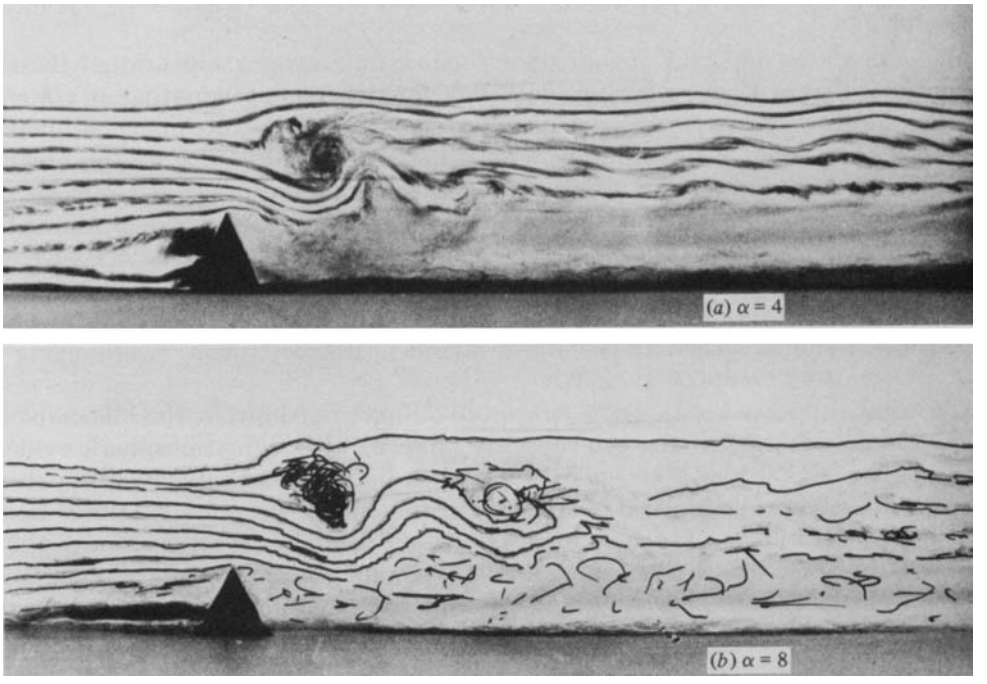


FIGURE 11. Dye streaks for $F = 0.4$.

Whether the 'tuning' is directly due to the three-dimensional effects of changing the spanwise aspect ratio of the hill or indirectly due to an effective increase in hill *length* caused by the longer recirculation region at larger $\alpha$ is unclear from the experiments. Analyses of the measurements of the distance $x_R$ to the first downstream centreline reattachment point (§ 3.3) did not lead to any identifiable trends in wave slope with, say, $x_R/\Lambda$; $x_R$ is evidently too simple a variable to use to correlate wave

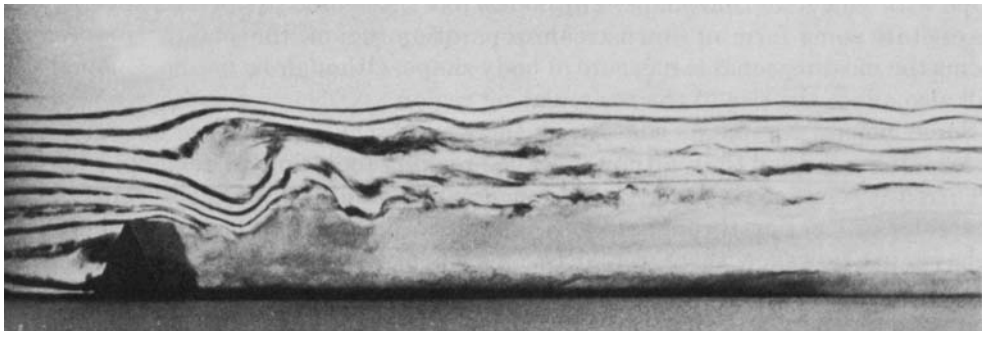

FIGURE 12. Same as figure 11(*a*), but taken later.

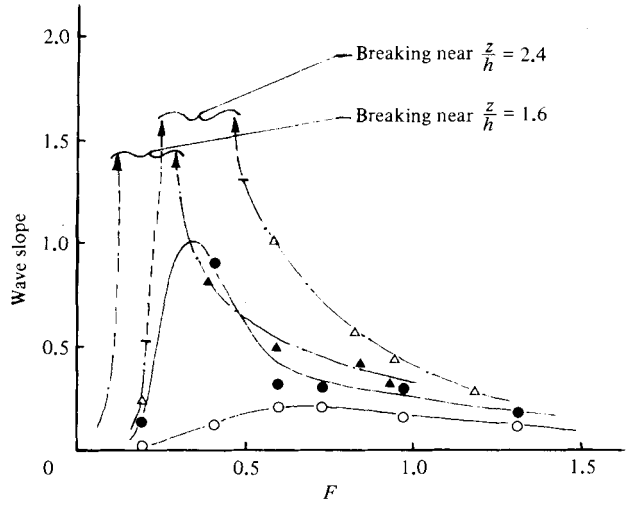


FIGURE 13. Wave slope of first wave shown by streamers at $z/h = 1.6$ (solid symbols) and $z/h = 2.4$ (open symbols): ○, ●, $\alpha = 1$; △, ▲, 8.

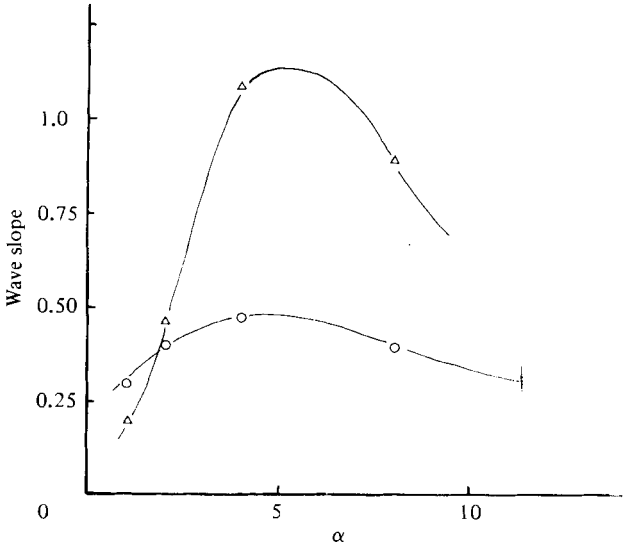


FIGURE 14. Slope of first lee wave for $z/h = 1.6$ streamer. ○, $F = 0.8$; △, 0.6.

slope with 'effective' hill shape. For bodies like those used in our experiment, which necessitate some form of downstream separation region, the spanwise aspect ratio seems the most reasonable measure of body shape, although the cross-sectional shape will also affect the size of the recirculating region.

Some general comments concerning the wave-breaking cases are in order. Visual observations showed that, although wave breaking took time to develop, once it had occurred it remained a fairly steady phenomenon and did not significantly change character or location throughout the remainder of the tow. (Ciné films confirm that behaviour.) However, there were occasions when wave breaking began immediately prior to the end of the tow. In these 'just-critical' cases, a steady flow may have taken longer to develop. Alternatively, they may have been 'just subcritical', but were affected by slightly changed flow conditions near the end of the tow, possibly caused by the reflection of upstream-propagating modes. In any event, the range of Froude numbers and hill aspect ratios that lead to wave breaking (suggested by figures 10 and 13) may be slightly underestimated. The evidence suggested, however, that, for these triangular-shaped ridges, wave breaking occurred if (very roughly) $\alpha > 3$ and $0.15 < F < 0.5$. In addition, the Froude-number range for wave breaking apparently increased as $\alpha$ increased, but further experiments would be needed to quantify the behaviour.

Finally, wave breaking can occur quite independently of the fully turbulent wake. Figure 12, a photograph taken a few seconds after the photograph in figure 11*a*), shows a distinct region of laminar flow between the rotor created by the wavebreaking and the eddy motions contained in the turbulent wake. This laminar region extends a considerable distance downstream. The stratification tends to suppress the wake turbulence, and a study of the far-wake flow would give little clue as to the presence of a breaking wave upstream. Similar behaviour has been observed in the atmosphere. In particular, the well-documented case of exceptionally strong mountain waves along the slope of the Colorado Rocky Mountains that occurred in January 1972 (Lilly & Zisper 1972; Lilly 1978) showed regions of strong turbulence near locations of maximum wave slope quite separated from turbulence at lower altitudes in the lee of the mountain.

### 3.3. *The wake flow*

#### 3.3.1. $F > 0.4$

Most of our deducations concerning the nature of the recirculating regions and wake flows were based on visual observations. Estimates of the average location of reattachment or separation points were most easily obtained by studying the movement of the small dye plumes injected into the wake. Since the flow was highly turbulent, still photographs were of little use; ciné pictures, however, generally confirmed the conclusions based on the many visual observations.

Although the recirculating region behind a three-dimensional obstacle cannot be properly regarded as a 'closed cavity' zone (e.g. Hunt *et al.* 1978), the distance $x_R$ to the downstream centreline reattachment point can often be used as a measure of the extent of the region of backflow. For neutral flow, $x_R$ generally increases with the body's spanwise aspect ratio, reaching some asymptotic value (as $\alpha \to \infty$) that depends on the body shape and the nature of the upstream flow. Figure 15 shows how $x_R$ varied with $\alpha$ in our study. The Reynolds number based on body height ranged from 4500 to 25000. Over this range, the upstream boundary layer was turbulent and any variation in $x_R/h$ with $Re$ was within the experimental uncertainty. For smaller values of $Re$, slight reductions in $x_R$ were noted. While no conclusive measurements were made for a two-dimensional ridge in neutral flow, $x_R/h$ in that

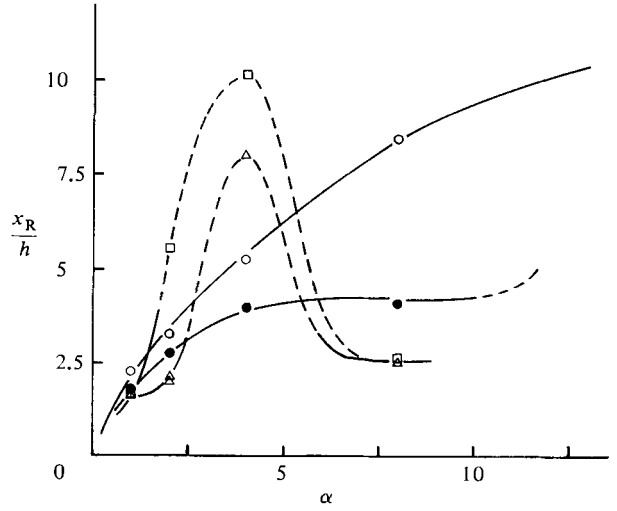


FIGURE 15. Location of downstream reattachment point on centreline: ○, $F = \infty$ (neutral flow); ●, 1.5; △, 1.0; □, 0.6.

case would probably have been about 12, somewhat smaller than that obtained for a two-dimensional flat plate, because the surface slope of the body just upwind of the separation point was smaller (Good & Joubert 1968; Castro & Fackrell 1981).

Based on the earlier work of HS, SBH and others, we anticipated that the addition of stable stratification, with the consequent presence of lee waves, would either promote early reattachment or delay reattachment, depending on the ratio $\Lambda/x_R$ of the lee-wavelength $\Lambda$ and $x_R$ in neutral flow. The results for $F = 0.6$, 1 and 1.5 are included in figure 15; these results confirm our expectation. For $F = 1.5$, the separated region was always considerably reduced in size, but, for $F = 0.6$ or 1, reattachment could be substantially delayed (at intermediate values of hill aspect ratio – those that generally yield maximum wave slopes; see § 3.2). In the latter cases, the low pressures under the first lee-wave downslope (Scorer 1978) were clearly insufficient to promote early reattachment, but the rising pressure under the first upslope *was* sufficient to delay reattachment. In the former cases reattachment usually occurred just upstream of the first trough in the lee-wave field, or earlier if the neutral flow $x_R/h$ was upstream of that. In the early-reattachment cases, $x_R/h$ depended much less on hill aspect ratio than it did in neutral flow, being controlled essentially by the lee-wave field.

For each hill, the variations that occurred in the flow patterns as $F$ was reduced were qualitatively fairly clear. Figure 16 presents 'composite' plots of the various flow features for $\alpha = 2$ and 8. The first change as $F$ was reduced was simply a reduction in the extent of the recirculating region, as discussed earlier. For $F < 1.5$, it was also possible to detect regions of slow-moving fluid downstream of reattachment and roughly one wavelength from the hill (i.e. under the first lee-wave crest); this is indicated in the figures. In some cases, the lee-wave field was sufficiently strong to promote a secondary separation and subsequent reattachment in these regions and occasionally a further region of slow-moving fluid could be seen under the second lee-wave crest (figure 16*a*, $F = 0.75$).

Figures 5(*b–d*) present surface streak patterns and illustrate another feature of the flow in the intermediate-Froude-number range ($0.4 < F < 1.0$). Recall that all the dye originated from a spanwise line at about $x/h = -10$. In the neutral case (figure 5*a*),

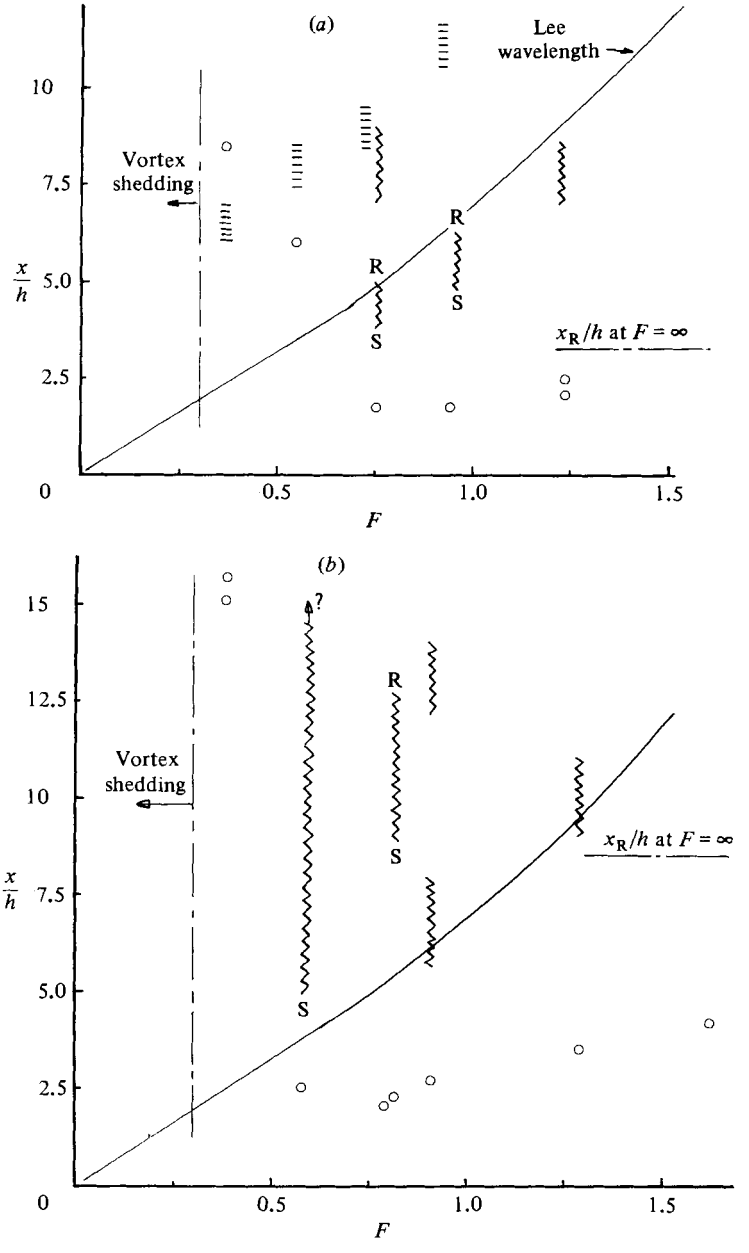


FIGURE 16. Features of the wake flow: ○, first centreline reattachment; ∧∧∧ regions of slow-moving fluid, or reversed if separation (S) and reattachment (R) are indicated; |||||| 'necking' location (see § 3.3.1 and figure 5). (*a*), $\alpha = 2$; (*b*) 8.

the downstream 'necking' occurred around the reattachment region and was very similar to that seen in wind-tunnel flow-visualization studies. The addition of stratification produced a marked change. Under stratified flow, the 'necking' occurred just beyond the first lee-wave trough; its location moved downstream with increasing $F$ (compare figures 5*b* and *c*). This was followed by strong spanwise three-dimensional separations on either side of the flow centreline; the limiting streamlines behind the necking position are much more clearly delineated than in the

neutral flow case and correspond to lines along which the spanwise velocity very close to the surface changes sign. Now stratification in the flow around three-dimensional bodies leads to baroclinically generated axial vorticity in the wake of the same sign as that produced by velocity shear in the upstream flow and/or separation from the faces (see e.g. Scorer 1978; Baines 1979*b*). It may be this reinforcement of axial vorticity that leads to such strong and stable spanwise separations in the near wake. This general feature was visible even for $\alpha = 4$, but a more careful examination of the phenomenon is needed. Visualization of multilevel dye streaks originating near, say, $y = \pm\frac{1}{2}W$, would have been helpful in this respect. We do not believe that there is any direct connection between these vortex motions and the curious 'cowhorn' eddies observed by Brighton (1978); such eddies were not noticed in the present studies.

3.3.2. $F < 0.4$

For very low Froude numbers the flow was constrained to move in horizontal planes, as anticipated. Very clear spanwise vortex shedding was also evident, even for $F$ as large as 0.3. Figure 17 (plate 1) shows shedding at $F = 0.2$ behind the $\alpha = 1$ ridge. In this case, red dye was injected from the hole in the rear face at $z/h = 0.5$ and yellow dye was injected from the hole nearer the top. Estimates of the Strouhal number $fW/\bar{U}$ based on shedding frequency, $f$, towing speed and hill *width* were between 0.14 and 0.18, without any apparent trends. These estimates are typical of values obtained in neutral flow past a flat plate or rectangular body, which is what the flow really 'sees' at such small $F$ (at least not too near $z = h$). The values are somewhat smaller, however, than those found by Brighton (1978) in studies of low-Froude-number flows past hemispheres, cones and truncated cylinders. HS found that vortex shedding ceased for $F \gtrsim 0.2$. Brighton also found that vortex shedding ceased for $F > 0.15$ and that this 'critical' Froude number did not depend on the Reynolds number for $Re > 500$. His maximum $Re$ was only $O(10^3)$, whereas in our study $Re$ was as large as $O(10^4)$ for the double-sized ($h = 18$ cm) $\alpha = 1$ ridge, which produced clear vortex shedding at $F = 0.2$ and rather weaker shedding at $F = 0.3$. In all cases, the vortex street took longer to develop as $F$ increased, until at $F = 0.4$ the wake merely 'meandered' in a way reminiscent of the flow behaviour in Morkovin's (1964) 'incipient Kármán range'.

An interesting feature of the vortex-shedding cases, shown very clearly by the ciné pictures, was that the convection speed $U_c$ of the vortices was greater at $z = \frac{1}{2}h$ than it was at $z = h$. Indeed, estimates from the films indicated that, at $z = \frac{1}{2}h$, $U_c$ was about equal to the free-stream speed (so that the vortices appeared stationary in the camera's frame of reference, which was fixed), whereas, at $z = h$, $U_c$ was only half the free-stream speed. A possible reason is provided by the nature of the upstream influence at low Froude number. Upstream-propagating columnar modes have a sinusoidal structure in the vertical (Wei *et al.* 1975), which must change the 'apparent' free-stream velocity at each height. Because the first-mode wavelength was about equal to $h$ at $F = 0.2$, there will certainly be a maximum and minimum upstream propagation velocity below $z = h$, but the size of the difference in convection velocities is surprising and perhaps not wholly attributable to this mechanism.

Finally, it should be emphasized that for $0.4 < F < 0.6$, where the flow was not strongly constrained to horizontal planes except perhaps far downstream where the stratification had damped out the near-wake turbulence, it was very difficult to obtain an adequate 'feel' for the processes occurring in the near wake. It was impossible

to view the wake as simply a perturbed version of the neutral flow case, as was done for $F > 0.6$. For example, at $F = 0.6$ and $\alpha = 8$, there was on average a centreline separation region subsequent to the early reattachment at $x/h = 2.5$ (see figure 16*b*), but no downstream reattachment was discernible and the flow was exceedingly complicated. It is well known that, in the case of flow past a two-dimensional bluff body remote from any boundary, the separated shear layers merge to form, on average, a 'free' stagnation point at about two body widths downstream (for cylinders or flat plates). In the present case, for $F = 0.4$ ($\alpha = 8$), where the flow was more nearly horizontal, the indicated reattachment point, at $x/h = 15$, could therefore really be thought of as the location of the free stagnation point (at about $x/W = 2$) behind a 'two-dimensional' body of width $W$.

## 4. Conclusions

Our experiments have confirmed the general effects indicated by previous theoretical and experimental studies of stratification on the flow over surface obstacles. In addition, our experiments have shown how the spanwise aspect ratio affects the flow. In particular, we have shown the following.

(1) The height of the upstream dividing streamline does not depend on the body shape and is in agreement with the implications of Sheppard's (1956) and Drazin's (1961) theories for $F \ll 1$, provided that upstream vortex motions are not significant. In our study, upstream vortex motions limited the range of agreement to $F \lesssim 0.3$, but for bodies with less steep upwind slopes and no upstream separations the '$1 - F$' rule is expected to hold up to $F = O(1)$. Snyder *et al.* (1982) recently confirmed that this result is, indeed, largely independent of body shape.

(2) The amplitude of the lee-wave field can be maximized by 'tuning' the body shape and $F$, as Crapper (1959, 1962) and Lilly & Klemp (1978) suggest. For the triangular-shaped ridges in our study, maximum wave amplitudes occurred at $F \approx 0.8$ for all $\alpha$, and maximum wave *slopes* occurred for $0.2 < F < 0.4$ and $\alpha \approx 5$.

(3) In the latter cases, steady wave-breaking can occur, and its location (in height) depends on $\alpha$ and $F$. Since Lilly & Klemp (1979) showed, for two-dimensional flow, that steep downslopes are much more effective than steep upslopes at producing strong lee waves, it is likely that the flow upstream of our particular bodies (which had steep upslopes) was much less significant in 'tuning' the flow's response than the changes in aspect ratio and/or the consequent changes in 'effective' downslope caused by interaction between the lee-wave field and the separated region. For body shapes which do not lead to inevitable separation, the actual slope of the body, particularly on the leeward side, is clearly an important parameter, as Lilly & Klemp (1979) demonstrated.

(4) As $F$ decreased from $\infty$, lee waves grew in amplitude and initially caused early reattachment, making the length of the recirculation zone much less dependent on $\alpha$ than in the neutral case. As $F$ was further reduced (from, say, 1.0), the strength of the lee waves (measured by the wave amplitude) decreased sufficiently to delay, rather than promote, reattachment. These conclusions are reminiscent of those of Hunt & Snyder (1980), who showed that the lee-wave field can control *separation* locations behind a smooth hill. In their study separation could also be boundary-layer controlled; in the present experiments it was fixed by geometry and the lee-wave field controlled reattachment behaviour. The implications for the full-scale situation of effluent sources downwind of steep hills are obvious although it must be borne in mind that the effects of nonlinear stratification, velocity shear or thin inversion layers in the upstream flow are likely to be at least as important as differences in body shape

(Scorer 1978). As Hunt & Snyder (1980) pointed out, there is clearly a need for experiments using density gradients that vary with height.

(5) The surface flow patterns in our experiments indicate that the baroclinically produced axial vorticity in the near wake reinforces that produced in the usual way by flow over a surface-mounted body sufficiently to promote strong three-dimensional separations downstream of early reattachment (for $0.6 < F < 1$, at least). Further experiments are needed to examine the effect of this apparent axial vorticity on the dispersion of plumes.

(6) For $F = 0.4$, the far wake 'meandered'; as $F$ was reduced, clear vortex shedding occurred. Strouhal numbers were independent of $F$, scaling simply on $U$ and the body width, and were similar to values (0.14–0.18) found for classic Kármán vortex streets behind two-dimensional bodies at high Reynolds numbers.

(7) The effects of upstream-propagating modes and actual blocking at the lowest levels, both of which are much less prominent in three- than in two-dimensional flows (see e.g. Baines' (1979*a*) study of the latter), were twofold in our experiments. First, stratification caused separation of the upstream boundary layer to depend much more on hill aspect ratio than it did in the neutral case. As $F$ was reduced, separation occurred earlier; this effect became more pronounced as $\alpha$ increased. However, this did not qualitatively affect the structure of the downstream flow. Secondly, our only explanation for the finding that the vortex-street convection speed varies dramatically with height is that the sinusoidal vertical structure of the upstream propagating modes cause variations in apparent free-stream velocity with height.

Although our results broadly conform to the collected wisdom concerning stratified flow over three-dimensional obstacles, further experiments would be useful. We made no attempt, for example, to examine the spanwise structure of the lee-wave field, to investigate the growth and decay of axial vorticity, or to find to what extent the downwind slope of the hill affects the flow for cases where separation remains fixed at the ridge top. However, the subject is so complicated that we close with Scorer's (1978) cautionary remark: 'There is almost no systematic way of discussing the flow behind a three-dimensional obstacle of arbitrary shape when separation occurs!' We believe, nevertheless that the various dominant phenomena can be usefully studied and think that the experiments reported here substantiate that belief.

We are grateful to the staff of the EPA Fluid Modeling Facility for their untiring help through all stages of the work. Particular thanks are due to Mr Roger Thompson for help with the photography and to Mr Joseph Smith for his hours at the pumps. Financial support for IPC was provided through an appointment as Visiting Assistant Professor, Department of Geosciences, North Carolina State University, under EPA Grant no. R805595, which is acknowledged with thanks.

## REFERENCES

Baines, P. G. 1977 Upstream influence and Long's model in stratified flows. *J. Fluid Mech.* **82**, 147–159.

Baines, P. G. 1979*a* Observations of stratified flow over two-dimensional obstacles in fluid of finite depth. *Tellus* **31**, 351–371.

Baines, P. G. 1979*b* Observations of stratified flow past three-dimensional barriers. *J. Geophys. Res.* **84**, 7834–7838.

Brighton, P. W. M. 1978 Strongly stratified flow past three-dimensional obstacles. *Q. J. R. Met. Soc.* **104**, 289–307.

Castro, I. P. & Fackrell, J. E. 1978 A note on two-dimensional fence flows, with emphasis on wall constraint. *J. Indust. Aero.* **3**, 1–20.

CORBY, G. A. & WALLINGTON, C. E. 1956 Air flow over mountains: the lee wave amplitude. *Q. J. R. Met. Soc.* **82**, 266.

CRAPPER, G. D. 1959 A three-dimensional solution for waves in the lee of mountains. *J. Fluid Mech.* **6**, 51–76.

CRAPPER, G. D. 1962 Waves in the lee of a mountain with elliptical contours. *Phil. Trans. R. Soc. Lond.* **A254**, 601–623.

DAVIES, R. E. 1969 The two-dimensional flow of a fluid of variable density over an obstacle. *J. Fluid Mech.* **36**, 127–143.

DRAZIN, P. G. 1961 On the steady flow of a fluid of variable density past an obstacle. *Tellus* **13**, 239–251.

GJEVIK, B. & MARTINSEN, T. 1978 Three-dimensional lee wave patterns. *Q. J. R. Met. Soc.* **104**, 947–957.

GOOD, M. C. & JOUBERT, P. N. 1968 Form drag of two-dimensional bluff plates immersed in turbulent boundary layers. *J. Fluid Mech.* **31**, 547–582.

HUNT, J. C. R., ABELL, C. J., PETERKA, J. A. & WOO, H. 1978 Kinematical studies of the flows around free or surface-mounted obstacles: applying topology to flow visualization. *J. Fluid Mech.* **86**, 179–200.

HUNT, J. C. R. & SNYDER, W. H. 1980 Experiments on stably and neutrally stratified flow over a model three-dimensional hill. *J. Fluid Mech.* **96**, 671–704.

KLEMP, J. B. & LILLY, D. K. 1978 Numerical simulation of hydrostatic mountain waves. *J. Atmos. Sci.* **35**, 78–107.

LILLY, D. K. 1978 Analysis of an intense mountain wave and aircraft turbulence. *J. Atmos. Sci.* **35**, 59–77.

LILLY, D. K. & KLEMP, J. B. 1979 The effects of terrain shape on nonlinear hydrostatic mountain waves. *J. Fluid Mech.* **95**, 241–261.

LILLY, D. K. & ZISPER, E. J. 1972 The front range windstorm of 11 January 1972 – a meteorological narrative. *Weatherwise* **25**, 56.

LONG, R. R. 1953 Some aspects of the flow of stratified fluids: I. A theoretical investigation. *Tellus* **5**, 42–57.

LONG, R. R. 1955 Some aspects of the flow of stratified fluids: III. continuous density gradients. *Tellus* **7**, 341–357.

LYRA, G. 1943 Theorie der stationären Leewellenströmung in freier Atmosphäre. *J. angew. Math. Mech.* **23**, 1.

MCINTYRE, M. E. 1972 On Long's hypothesis of no upstream influence in uniformly stratified or rotating fluid. *J. Fluid Mech.* **52**, 209–243.

MILES, J. W. (with appendix by HUPPERT, H. E.) 1968 Lee waves in a stratified flow. Part 2. Semicircular obstacle. *J. Fluid Mech.* **33**, 804–814.

MORKOVIN, M. V. 1964 Flow around circular cylinders – a kaleidoscope of challenging fluid phenomena. In *Proc. ASME Symp. on Fully Separated Flows*, pp. 102–118.

QUENEY, P. 1948 The problem of airflow over mountains: a summary of theoretical studies. *Bull. Am. Met. Soc.* **29**, 16.

SCORER, R. S. 1978 *Environmental Aerodynamics*. Wiley.

SHEPPARD, P. A. 1956 Airflow over mountains. *Q. J. R. Met. Soc.* **82**, 528–529.

SMITH, R. B. 1980 Linear theory of stratified hydrostatic flow past an isolated mountain. *Tellus* **32**, 348–364.

SNYDER, W. H., BRITTER, R. E. & HUNT, J. C. R., 1980 A fluid modeling study of the flow structure and plume impingement on a three-dimensional hill in stably stratified flow. In *Proc. 5th Intl Conf. on Wind Engng* (ed. J. E. Cermak), vol. 1, pp. 319–329. Pergamon.

SNYDER W. H., THOMPSON, R. S., ESKRIDGE, R. E., LAWSON, R. E., CASTRO, I. P., LEE, J. T., HUNT, J. C. R. & OGAWA, Y. 1982 The structure of strongly stratified flow over hills: dividing-streamline concept. Submitted to *J. Fluid Mech.*

THOMPSON, R. S. & SNYDER, W. H. 1976 EPA fluid modeling facility. In *Proc. Conf. on Environ. Modeling and Simulation. Environ. Prot. Agcy Rep.* EPA 600/9-76-016, Wash, D.C., July.

WEI, S. N., KAO, T. W. & PAO, H. P. 1975 Experimental study of upstream influence in the two-dimensional flow of a stratified fluid over an obstacle. *Geophys. Fluid Dyn.* **6**, 315–336.

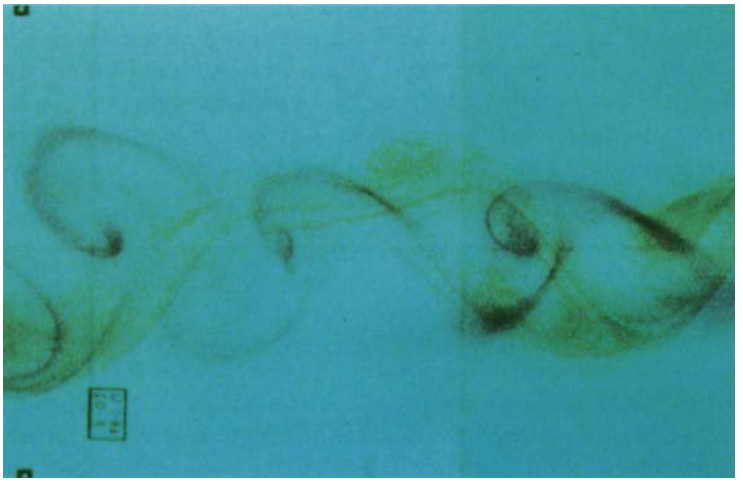

FIGURE 17. Vortex shedding at $F = 0.2$ behind $\alpha = 1$ ridge. Red dye injected at $z/h = 0.5$; yellow dye at $z/h = 0.9$. The body is moving from right to left and is some way to the left of the left-hand margin. (Photograph reproduced from ciné film.)